

Spectral Optimization of Torsional Eigenvalues for a Nonhomogeneous Fish-Bone Plate with Piers

Original

Spectral Optimization of Torsional Eigenvalues for a Nonhomogeneous Fish-Bone Plate with Piers / Berchio, E., Garrione, M., Patriarca, C.. - In: APPLIED MATHEMATICS AND OPTIMIZATION. - ISSN 0095-4616. - 93:1(2026), pp. 1-28. [10.1007/s00245-025-10312-z]

Availability:

This version is available at: 11583/3008360 since: 2026-03-09T09:03:52Z

Publisher:

Springer

Published

DOI:10.1007/s00245-025-10312-z

Terms of use:

This article is made available under terms and conditions as specified in the corresponding bibliographic description in the repository

Publisher copyright

(Article begins on next page)



Spectral Optimization of Torsional Eigenvalues for a Nonhomogeneous Fish-Bone Plate with Piers

Elvise Berchio¹ · Maurizio Garrione² · Clara Patriarca³

Received: 18 June 2025 / Accepted: 15 August 2025
© The Author(s) 2025

Abstract

Motivated by stability issues for suspension bridges, the analysis focuses on the maximization of the torsional eigenvalues of a nonhomogeneous multi-span fish-bone plate with respect to the mass density. The incorporation of internal piers significantly impacts the spectral properties of the system. After a general spectral theorem, a characterization of the densities maximizing the first and the second torsional eigenvalue is provided, starting from the corresponding results for the nonhomogeneous Dirichlet problem. In the case where the mass of the central span is equal to its length, more explicit insight is then given, taking into account the role of the position of the piers and discussing the scenario for higher-order eigenvalues, as well.

Keywords Optimization · Fish-bone plate · Nonhomogeneous beam · Multiply hinged conditions · Torsional eigenvalues

Mathematics Subject Classification Primary 34L15 · 74K20

✉ Elvise Berchio
elvise.berchio@polito.it

Maurizio Garrione
maurizio.garrione@polimi.it

Clara Patriarca
clara.patriarca@ulb.be

¹ Dipartimento di Scienze Matematiche, Politecnico di Torino, Corso Duca degli Abruzzi 24, 10129 Torino, Italy

² Dipartimento di Matematica, Politecnico di Milano, Piazza Leonardo da Vinci, 32, 20133 Milano, Italy

³ Departement de Mathématique, Université Libre de Bruxelles, Boulevard du Triomphe, Acc. 2, 1050 Ixelles, Belgium

1 Introduction and Mathematical Model

In the last years, there have been advances in the theoretical understanding of the coupled dynamics involving vertical and torsional oscillations of suspension bridges, as the result of a growing interest for the corresponding PDE models (see [1] for a very rich compendium of results). In many cases, these consist in two coupled evolution equations, one of beam type for the vertical oscillations and one of wave type for the torsional ones. The role of the (vertical and torsional) *frequencies* of the active oscillation modes was recognized as crucial for the stability since the origins of such a theoretical investigation, dating back to the famous Tacoma Narrows Bridge collapse in 1940. In that occasion, the *second* torsional mode (in mathematical terms, the second torsional eigenfunction) had suddenly become active due to a transfer of energy from a vertical oscillation with a high number of humps (nine or ten). Subsequently, special attention was then devoted to prevent such an energy transfer towards the second torsional mode, which is particularly dangerous for the structure due to its *twisting* effect.

From a mathematical perspective, a possible way of avoiding the onset of motions concentrated on the second torsional mode is to act on the characteristic parameters of the structure (e.g., the mass distribution and the shape of the deck) so as to augment as much as possible the energy which is needed for their appearance. Since such an energy is directly proportional to the second torsional eigenvalue, a natural attempt may be to design the structure in order to increase such an eigenvalue to the maximum extent. In this work, we focus primarily on the effect of the *mass distribution* along the structure; the position of the piers and the amount of mass in each span are also taken into account.

The starting point of our investigation is represented by the fish-bone model introduced in [2], in its multiply hinged version developed in [3, Chapter 5] (and called *degenerate plate* therein), see Fig. 1. It is a highly simplified mathematical model that nevertheless retains the essential features of the structures under consideration. In particular, this simplicity makes it suitable for conducting an in-depth theoretical analysis.

According to this configuration, the deck of the bridge is composed by a central beam (the dashed midline in Fig. 1) of (normalized) length 2π , which is identified with the interval $I := (-\pi, \pi)$ and is hinged at the endpoints, and by a continuum of

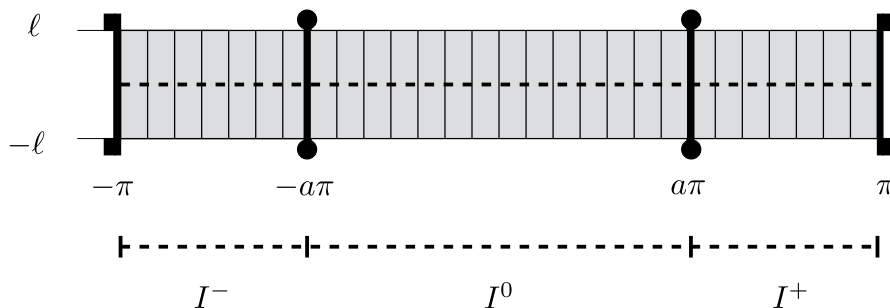


Fig. 1 The multiply hinged fish-bone plate

cross-sections of normalized half-length 1 - one for each $x \in I$ - which are free to rotate around their barycenter, placed on I . Moreover, as in [3], for fixed $a \in (0, 1)$ the two cross-sections at position $x = \pm a\pi$ are assumed to remain still, in order to model the presence of internal piers (towers). The deriving *multiply span* structure is then called a *multiply hinged fish-bone* and is made of three different *spans*: the *central* one $I^0 = (-a\pi, a\pi)$ and the *side* (or *lateral*) ones $I^- := (-\pi, -a\pi)$ and $I^+ := (a\pi, \pi)$, these two having the same length by assumption. From a theoretical point of view, the main effect of the internal piers is to lower the regularity of both vertical and torsional eigenfunctions, as pointed out in [4]: the vertical eigenfunctions are only C^2 , while the torsional ones are only continuous. This makes the functional setting for the multi-span problem and the related spectral analysis more delicate.

In order to deal with a more realistic - yet simplified - model, we here consider a *nonhomogeneous* multiply hinged fish-bone plate, allowing for a nonconstant mass distribution, aiming to investigate the consequences on the torsional eigenvalues (the analysis of vertical eigenvalues was carried out in [5] but within a model with one degree of freedom, where torsional motions were not taken into account). Specifically, we aim to determine the mass distribution which *maximizes* a selected torsional eigenvalue (typically, the second one). This is motivated, e.g., by the results in [3, Chapter 4], where the linear stability analysis in the constant density case revealed that the higher the torsional frequency, the higher the energy threshold of linear instability which triggers the corresponding torsional mode. The difficulty of the spectral optimization problems considered here primarily arises from the presence of the internal piers, which create additional internal conditions that prevent the application of classical optimization results for weighted eigenvalue problems, such as those contained in [6]. Moreover, unlike the original fish-bone model, *multiple* eigenvalues may here appear (cf. [4, Section 4]), significantly impacting the spectral properties of the system (see Section 3).

The paper is organized as follows: we first define the torsional modes in the nonhomogeneous setting and provide some general results about the considered spectral optimization problem (Section 2), such as the existence of a sequence of eigenvalues and their relationships with the nonhomogeneous Dirichlet eigenvalues on each span. In Section 3, we identify a class of *admissible* densities and we show that the maximization problem is always solvable in such a class, for any torsional eigenvalue. By carefully exploiting some classical results by Krein [7] for the nonhomogeneous Dirichlet problem on an interval, we then provide maximization results for the first and for the second torsional eigenvalue, characterizing the corresponding maximizing densities. In Section 4, we examine the noteworthy case in which the mass distributed along the central span is equal to its length. This allows for more readable results and enables a more comprehensive analysis, including the optimization of the subsequent torsional eigenvalues and some considerations about the role of the positioning of the piers. A physical interpretation of the results is provided in Remark 4.7. We finally mention that the effects of the density distribution on the stability of partially hinged plates (without piers) modeling bridges have been discussed, e.g., in [8–12], see also [13] for a discussion from the point of view of shape optimization. Broadly speaking, the problems considered in the present paper fall within the wide

research field involving spectral optimization for *composite membranes and plates*, see for instance [14–25] and, again, the monograph [6] (and the references therein).

2 The Nonhomogeneous Torsional Eigenvalue Problem

In this section, having in mind the fish-bone configuration described in the Introduction (see Fig. 1), we provide general results for the corresponding (second order) torsional eigenvalue problem under the assumption that the mass distribution along the structure is *nonhomogeneous*.

Precisely, for given $0 < \alpha < 1 < \beta$, we consider the following class of density distributions:

$$P_{\alpha,\beta} := \left\{ p \in L^\infty(I) : \int_I p dx = 2\pi, \alpha \leq p \leq \beta \text{ and } p(x) = p(-x) \text{ a.e. in } I \right\}. \quad (1)$$

The integral condition in (1) represents the preservation of the total mass, which is a natural physical constraint and allows one to compare the results for different mass distributions. The constants α and β act as (lower and upper) bounds for the density, which is symmetric with respect to the center of the beam by assumption (notice that also the position of the piers is assumed to be symmetric).

When dealing with the dynamics of the deck of a suspension bridge, a central role is played by the oscillating modes of the fish-bone plate that models the structure. Since the related PDE system is of beam-wave type, we can distinguish between the *vertical* (related to the beam equation in the system) and the *torsional* (related to the wave equation therein) eigenfunctions, respectively solving a fourth order and a second order stationary eigenvalue problem. As explained in the Introduction, here we are interested in the *torsional* modes, which can be expressed through the eigenfunctions of the problem

$$\begin{cases} -\eta''(x) = kp(x)\eta(x) & k \in \mathbb{R}, x \in I \\ \eta(\pm\pi) = \eta(\pm a\pi) = 0. \end{cases} \quad (2)$$

In the case of a constant density $p \equiv 1$, it was highlighted in [4] that the presence of the internal piers produces a loss in the regularity of such functions; more precisely, the *torsional* eigenfunctions are only *continuous* and hence - since the continuity is already guaranteed by the no displacement condition in correspondence of the piers - each span behaves independently of the others. In fact, the considerations we will draw about the torsional eigenfunctions and the maximization of the torsional eigenvalues will often rely on a comparison between the Dirichlet problems considered on I^\pm or I^0 only (recall Fig. 1).

As a general rule of notation, henceforth we use no superscripts when referring to the entire interval I (in the previously introduced framework), while we adopt the superscripts⁻, ⁰ and⁺, respectively, when restricting our attention on I^- , I^0 and I^+ ; when possible, we also use the superscript[±] in order to deal, at the same time, with I^- and I^+ , this often being possible thanks to the symmetry of both the

piers and the density. Sometimes it will be useful to pass from a single span to the whole I via (trivial) extension or to restrict from I to a single span. Denoting by $H_0^1(I)$, $H_0^1(I^\pm)$ and $H_0^1(I^0)$ the usual Sobolev spaces of H^1 -functions with zero trace at the endpoints, we set

$$W(I) := \{w \in H_0^1(I) : w(\pm a\pi) = 0\}.$$

Clearly, $W(I) \subset C(\bar{I})$. Moreover, the extension operators

$$E^\pm : H_0^1(I^\pm) \rightarrow W(I), \quad E^0 : H_0^1(I^0) \rightarrow W(I)$$

$$w \mapsto E^\pm(w) = \begin{cases} w(x) & x \in I^\pm \\ 0 & x \in I \setminus I^\pm \end{cases} \quad w \mapsto E^0(w) = \begin{cases} w(x) & x \in I^0 \\ 0 & x \in I \setminus I^0 \end{cases}$$

are all well defined and continuous; vice versa, if $\eta \in W(I)$, the restrictions $\eta|_{I^\pm}$ and $\eta|_{I^0}$ belong, respectively, to $H_0^1(I^\pm)$ and $H_0^1(I^0)$. In the following, for brevity, $E^-(w)$, $E^0(w)$ and $E^+(w)$ will all be indicated by the same symbol \tilde{w} .

With these preliminaries, in this section we give results about the torsional eigenfunctions for a nonhomogeneous fish-bone plate with nonconstant density $p \in P_{\alpha,\beta}$. We first formalize the notion of (weak) *solution* of (2), that we will refer to in the following.

Definition 2.1 Let $p \in P_{\alpha,\beta}$ be fixed. We say that η is a *torsional eigenfunction* associated with the (torsional) eigenvalue $k \in \mathbb{R}$ if $\eta \in W(I)$ and η solves (2) in weak sense, that is,

$$\int_I \eta' w' dx = k \int_I p(x) \eta w dx \quad \forall w \in W(I). \tag{3}$$

Notice that the torsional eigenvalues are actually all *strictly positive*, as can be seen by taking $w = \eta$ in (3) (thanks to the fact that p is positive).

In order to provide results for (3), it is useful to consider separately the Dirichlet problems

$$\begin{cases} -(\eta^\pm)''(x) = k^\pm p(x)|_{I^\pm} \eta^\pm(x), & x \in I^\pm \\ \eta^\pm(-\pi) = 0 = \eta^\pm(-a\pi) \end{cases} \quad \text{and} \tag{4}$$

$$\begin{cases} -(\eta^0)''(x) = k^0 p(x)|_{I^0} \eta^0(x), & x \in I^0 \\ \eta^0(\pm a\pi) = 0; \end{cases}$$

we point out that, in view of the assumptions on p , the solutions of each of the problems in (4) enjoy H^2 -regularity on the considered span. From the standard theory of linear eigenvalue problems, we then have the following.

Proposition 2.2 *The eigenvalues of each of the problems in (4) are simple and can be ordered into strictly increasing sequences $\{k_i^\pm\}_{i \in \mathbb{N}_+}$ and $\{k_i^0\}_{i \in \mathbb{N}_+}$, respec-*

tively. Moreover, $k_i^-(p) = k_i^+(p)$ for all $i \in \mathbb{N}_+$ and, denoting by $\eta_i^- \in H_0^1(I^-)$ and $\eta_i^+ \in H_0^1(I^+)$ the corresponding eigenfunctions, it is possible to choose $\eta_i^+(x) = \eta_i^-(-x)$ for every $x \in I^+$.

The second part of the statement follows from the symmetry of the considered beam and from the parity of the density p . Proposition 2.2 allows us to determine the eigenvalues of problem (3), as follows.

Theorem 2.3 *The eigenvalues of (3) may be either simple, double or triple and are given by*

$$\{k_i(p)\}_{i \in \mathbb{N}_+} = \{k_i^\pm(p|_{I^\pm}), k_i^0(p|_{I_0})\}_{i \in \mathbb{N}_+}.$$

Concerning the first eigenvalue, it holds that

$$k_1(p) = \min\{k_1^\pm(p|_{I^\pm}), k_1^0(p|_{I_0})\}$$

and one of the following occurs:

- (i) $k_1(p) = k_1^\pm(p|_{I^\pm}) = k_1^0(p|_{I_0})$, so that k_1 has multiplicity three. In this case, three linearly independent eigenfunctions associated with k_1 are given by $\{\tilde{\eta}_1^-, \tilde{\eta}_1^0, \tilde{\eta}_1^+\}$;
- (ii) $k_1(p) = k_1^\pm(p|_{I^\pm}) < k_1^0(p|_{I_0})$, so that k_1 has multiplicity two. In this case, two linearly independent eigenfunctions associated with k_1 are given by $\{\tilde{\eta}_1^-, \tilde{\eta}_1^+\}$;
- (iii) $k_1(p) = k_1^0(p|_{I_0}) < k_1^\pm(p|_{I^\pm})$, so that k_1 is simple. In this case, the first eigenfunction is given by $\tilde{\eta}_1^0$.

We refer to formula (23) below for sharp bounds regarding the eigenvalues $k_i^\pm(p|_{I^\pm})$ and $k_i^0(p|_{I_0})$ and to Fig. 6 for their visualization in dependence on the parameter a , in the case where the mass of the central span matches its length.

Proof of Theorem 2.3 Let k be an eigenvalue of (3), with corresponding (weak) eigenfunction $\eta_k \in W(I)$, and, for the sake of readability, set $\eta_k^\pm = \eta_k|_{I^\pm}$ and $\eta_k^0 = \eta_k|_{I^0}$. By the definition of $W(I)$, we have that $\eta_k^\pm \in H_0^1(I^\pm)$, $\eta_k^0 \in H_0^1(I^0)$. Moreover, since η_k satisfies (3), it holds

$$\int_{I^\pm} (\eta_k^\pm)' w' dx = \int_I \eta_k' \tilde{w}' dx = \int_I p(x) \eta_k \tilde{w} dx = \int_{I^\pm} p(x) \eta_k^\pm w \quad \forall w \in H_0^1(I^\pm),$$

$$\int_{I^0} (\eta_k^0)' w' dx = \int_I \eta_k' \tilde{w}' dx = \int_I p(x) \eta_k \tilde{w} dx = \int_{I^0} p(x) \eta_k^0 w \quad \forall w \in H_0^1(I^0),$$

hence η_k^\pm satisfies (4)₁ with $k^\pm = k$ and η_k^0 satisfies (4)₂ with $k^0 = k$.

Conversely, if k^\pm is an eigenvalue of (4)₁ with eigenfunction $\eta^\pm \in H_0^1(I^\pm)$,

$$\int_I (\tilde{\eta}^\pm)' w' dx = \int_{I^\pm} (\eta^\pm)' (w|_{I^\pm})' dx = \int_{I^\pm} p(x) \eta^\pm w|_{I^\pm} dx = \int_I p(x) \tilde{\eta}^\pm w \quad \forall w \in W(I),$$

showing that the trivial extension $\tilde{\eta}^\pm$ satisfies (3) for $k = k^\pm$. The same holds for the eigenfunctions and the eigenvalues of problem (4)₂.

As for the final part of the statement, it follows straightly from the previous considerations, recalling that one has $k_i^-(p|_{I^-}) = k_i^+(p|_{I^+})$ for all $i \in \mathbb{N}_+$ and hence each eigenvalue can be either simple (when it is an eigenvalue of problem (4)₂ only), double (when it is an eigenvalue of the two problems (4)₁ but not of (4)₂) or triple (when it solves each of the problems in (4)). By definition, the first eigenvalue $k_1(p)$ is the least among all the eigenvalues of the problems in (4).

Remark 2.4 Notice that the eigenfunctions of (3) coincide with the trivial extensions of the eigenfunctions of the Dirichlet problems in (4), in line with the previous observation that each span behaves separately. For this reason, they are not C^1 on the whole I , in general. However, by a similar argument as the one in [26, Lemma 2.2], they are continuous on I and C^1 on each subset of I^\pm and I^0 where p is continuous. In particular, simple eigenvalues are always associated with eigenfunctions that vanish on the side spans.

3 Spectral Optimization

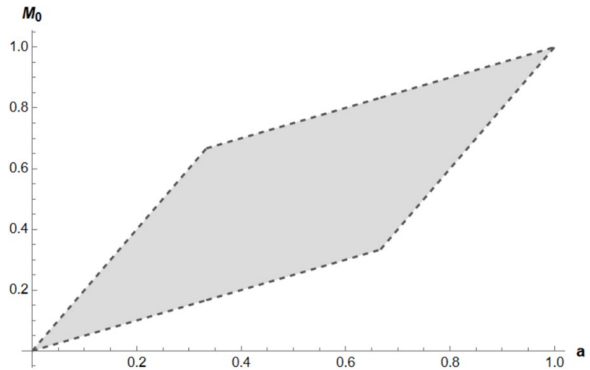
In this section, we investigate the densities which maximize the torsional eigenvalues of a nonhomogeneous fish-bone plate with symmetric piers. For the sake of readability, our analysis will focus only on the first and on the second eigenvalue, which can be considered as the most “dangerous” ones in relation to the stability of the structure, as recalled in the Introduction. The optimization of higher torsional eigenvalues is considered in Section 4, in the case in which the mass distributed along the central span is equal to its length.

As a first issue, in the applications it is reasonable to establish a priori the amount of material to be located in each span. We thus introduce a further parameter $M^0 \in (0, 1)$, representing the share of the total mass located in the central span I^0 , that in our analysis will be assumed to be equal to $2\pi M^0$. More precisely, for fixed $0 < \alpha < 1 < \beta$ we define the set

$$\Omega_{\alpha,\beta} := \{(a, M^0) : 0 < a < 1 \text{ and } \max\{\alpha a, 1 - (1 - a)\beta\} < M^0 < \min\{\beta a, 1 - (1 - a)\alpha\}\} \quad (5)$$

(see Fig. 2), representing the set of admissible choices of (a, M^0) in our framework. Indeed, in view of (1), the mass concentrated on the lateral spans is at least (resp., at most) equal to $2\pi(1 - a)\alpha$ (resp., $2\pi(1 - a)\beta$), hence M_0 must satisfy $2\pi M^0 \leq 2\pi(1 - (1 - a)\alpha)$ (resp., $2\pi M^0 \geq 2\pi(1 - (1 - a)\beta)$); on the other hand, since the lower (resp., upper) bound on p , prescribed in (1), is equal to α (resp., β), it must be $2\pi M^0 \geq 2\pi\alpha a$ (resp., $2\pi M^0 \leq 2\pi\beta a$). Now, if one of the inequalities for M^0 in (5) was an equality, it would be $p \equiv \alpha$ or $p \equiv \beta$ (a.e.) either on the central or on the lateral spans; consequently, the optimization problem would be solved by simply optimizing the eigenvalue of a weighted Dirichlet problem on a single interval (see, e.g., [6, Chapter 9]); this is the reason why we are excluding the equality cases in (5).

Fig. 2 The set $\Omega_{\frac{1}{2}, 2}$



Fixed $(a, M^0) \in \Omega_{\alpha, \beta}$, we thus work with the class of densities

$$\bar{P}_{\alpha, \beta} := \left\{ p \in P_{\alpha, \beta} : \int_{I^0} p(x) dx = 2\pi M^0 \right\};$$

of course, from (1), any $p \in \bar{P}_{\alpha, \beta}$ is such that $\int_{I^\pm} p(x) dx = \pi(1 - M^0)$. For every $i \in \mathbb{N}_+$ and every $p \in \bar{P}_{\alpha, \beta}$, we then consider the eigenvalues $\{k_i\}_{i \in \mathbb{N}_+}$ of (3); henceforth, we assume that

$$k_i(p) < k_{i+1}(p) \quad \text{for every } p \in P_{\alpha, \beta} \text{ and every } i \in \mathbb{N}_+,$$

namely we count the eigenvalues with multiplicity.

Our main target is to study the maximum problems

$$\Lambda_i = \Lambda_i(a, M^0) := \max_{p \in \bar{P}_{\alpha, \beta}} k_i(p). \tag{6}$$

We start by showing that Λ_i is well defined.

Proposition 3.1 *Let $0 < \alpha < 1 < \beta$ and $(a, M^0) \in \Omega_{\alpha, \beta}$ fixed. Then, for every $i \in \mathbb{N}_+$ problem (6) admits a solution, i.e., there exists $\bar{p}_i \in \bar{P}_{\alpha, \beta}$ such that $k_i(\bar{p}_i) = \Lambda_i$.*

Proof In view of Theorem 2.3, for every $i \in \mathbb{N}_+$ the map $k_i : \bar{P}_{\alpha, \beta} \ni p \mapsto k_i(p) \in \mathbb{R}$ is continuous with respect to the weak* convergence of densities, thanks to the fact that this is true for the eigenvalues of the Dirichlet problems in (4), cf. [6, Theorem 9.1.3]. On the other hand, following for instance the argument in [5, Lemma 6.4], it is immediately shown that the set $\bar{P}_{\alpha, \beta}$ is compact in the weak* topology of L^∞ . The conclusion follows.

In Subsections 3.2 and 3.3, we provide explicit information about the maximum value in (6) and the shape of the corresponding maximizing density. To this end, in

the next subsection we preliminarily recall some classical facts about the Dirichlet eigenvalue problem with nonhomogeneous density.

3.1 The Dirichlet Eigenvalue Problem with Nonhomogeneous Density: Spectral Optimization

We here briefly recall some classical results [7] for the Dirichlet eigenvalue problems in (4), adapted to our setting. To this end, fixed $(a, M^0) \in \Omega_{\alpha,\beta}$, we consider classes of densities which, on each span, obey mass constraints which are consistent with the definition of $\bar{P}_{\alpha,\beta}$. Namely, we set

$$P_{\alpha,\beta}^\pm := \{p \in L^\infty(I^\pm) : \int_{I^\pm} p dx = \pi(1 - M^0), \alpha \leq p \leq \beta \text{ a.e. in } I^\pm\} \quad (7)$$

and

$$P_{\alpha,\beta}^0 := \{p \in L^\infty(I^0) : \int_{I^0} p dx = 2\pi M^0, \alpha \leq p \leq \beta \text{ and } p(x) = p(-x) \text{ a.e. in } I^0\}. \quad (8)$$

Indeed, for every $p \in \bar{P}_{\alpha,\beta}$, it is clear that $p|_{I^\pm} \in P_{\alpha,\beta}^\pm$ and $p|_{I^0} \in P_{\alpha,\beta}^0$. Among the densities defined in (7) and (8), we will see that a crucial role will be played by *bang-bang* functions assuming alternatively the sole values α and β and having two symmetric jumps on each span. To provide their explicit expression, it is convenient to define the two numbers

$$b = \frac{1 - M^0 - (1 - a)\alpha}{2(\beta - \alpha)} \in \left(0, \frac{1 - a}{2}\right) \quad \text{and} \quad c = \frac{a\beta - M^0}{\beta - \alpha} \in (0, a), \quad (9)$$

which are related to the location of the density jumps so as to fulfill all the previously discussed mass constraints (see (10)). For every $i \in \mathbb{N}_+$, we then define the piecewise constant functions $p_i^\pm : I^\pm \rightarrow \mathbb{R}, p_i^0 : I^0 \rightarrow \mathbb{R}$ as

$$p_1^+(x) := \begin{cases} \beta & \text{for } x \in (a\pi, (a+b)\pi) \\ \alpha & \text{for } x \in ((a+b)\pi, (1-b)\pi) \\ \beta & \text{for } x \in ((1-b)\pi, \pi), \end{cases} \quad p_1^-(x) := p_1^+(-x), \quad p_1^0(x) := \begin{cases} \beta & \text{for } x \in (-a\pi, -c\pi) \\ \alpha & \text{for } x \in (-c\pi, +c\pi) \\ \beta & \text{for } x \in (c\pi, a\pi), \end{cases} \quad (10)$$

$$p_i^\pm(x) = p_1^\pm(\pm ix - (i-1)a\pi) \text{ for } x \in \left(a\pi, a\pi + \frac{(1-a)\pi}{i}\right), \text{ extended to } I^\pm \text{ by } \frac{|I^\pm|}{i} \text{-periodicity.} \quad (11)$$

$$p_i^0(x) = p_1^0(ix + (i-1)a\pi) \text{ for } x \in \left(-a\pi, -a\pi + \frac{2a\pi}{i}\right), \text{ extended to } I^0 \text{ by } \frac{|I^0|}{i} \text{-periodicity.} \quad (12)$$

For $i \geq 2$, such functions are obtained by juxtaposing several copies of a piecewise constant function taking the value β at the endpoints of the considered interval and α in the middle, with two symmetric jumps; by construction, it holds that $p_i^\pm \in P_{\alpha,\beta}^\pm$ and $p_i^0 \in P_{\alpha,\beta}^0$ for every $i \in \mathbb{N}_+$. In Fig. 3, as an example, for $\alpha = 0.8$, $\beta = 0.2$ and $M^0 = 0.4$ we depict, respectively, the graphs of p_1^- (orange), p_1^0 (black),

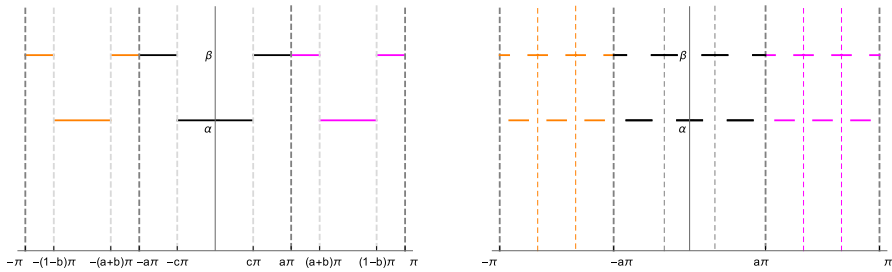


Fig. 3 Examples of graphs of the densities defined in (10), (11) and (12)

p_1^+ (magenta) (left picture) and p_3^- (orange), p_3^0 (black), p_3^+ (magenta) (right picture), juxtaposing them so as to obtain the graph of a single overall function over the entire I for the sake of synthesis.

We now rewrite in our setting some results provided in [7], see also [6, Theorem 9.3.3], for the three maximization problems

$$\Lambda_i^\pm = \Lambda_i^\pm(a, M^0) := \max_{p \in P_{\alpha, \beta}^\pm} k_i^\pm(p) \quad \text{and} \quad \Lambda_i^0 = \Lambda_i^0(a, M^0) := \max_{p \in P_{\alpha, \beta}^0} k_i^0(p), \tag{13}$$

where $k_i^\pm(p)$ and $k_i^0(p)$ are the eigenvalues of (4)₁ and (4)₂, respectively.

Proposition 3.2 [7, Theorem 5]. *For every $i \in \mathbb{N}_+$, it holds*

$$\Lambda_i^\pm = \frac{4i^2}{\alpha[(1-a-2b)\pi]^2} \omega^2 \left(\frac{\beta}{\alpha}, \frac{2b}{1-a-2b} \right) \quad \text{and} \quad \Lambda_i^0 = \frac{i^2}{\alpha(c\pi)^2} \omega^2 \left(\frac{\beta}{\alpha}, \frac{a-c}{c} \right), \tag{14}$$

where b, c are defined in (9) and $\omega(s, t) : (0, \infty)^2 \rightarrow \left(0, \frac{\pi}{2}\right)$ is the least positive root of the equation

$$\tan(\omega) = \sqrt{s} \cotan(\sqrt{st}\omega). \tag{15}$$

Moreover, Λ_i^\pm and Λ_i^0 are uniquely achieved, respectively, by the densities p_i^\pm and p_i^0 defined in (11)-(12).

For every $(s, t) \in (0, \infty)^2$, $\omega(s, t)$ is indeed well defined, since both $g_{\tan} : (0, \pi/2) \rightarrow (0, \infty)$ and $g_{\cotan} : \left(0, \frac{\pi}{2\sqrt{st}}\right) \rightarrow (0, \infty)$, respectively defined by $g_{\tan}(\omega) = \tan(\omega)$ and $g_{\cotan}(\omega) = \sqrt{s} \cotan(\sqrt{st}\omega)$, are nonnegative and monotone functions (increasing and decreasing, respectively) having range equal to $(0, \infty)$. Hence, the graphs of g_{\tan} and g_{\cotan} intersect exactly once in the interval $\left(0, \min \left\{ \frac{\pi}{2}, \frac{\pi}{2\sqrt{st}} \right\} \right)$; it follows that

$$\omega(s, t) \in \left(0, \min \left\{ \frac{\pi}{2}, \frac{\pi}{2\sqrt{st}} \right\} \right) \quad \text{for every } (s, t) \in (0, \infty)^2. \tag{16}$$

The function ω implicitly defined by (15) satisfies some asymptotic properties which we list in the following proposition and will be exploited in Section 4.1; to this end, for any $t > 0$ we denote by $\omega_0^t \in \left(0, \frac{\pi}{2}\right)$ the unique number for which $\omega_0^t \tan(\omega_0^t) = \frac{1}{t}$.

Proposition 3.3 *The following hold:*

$$\lim_{t \rightarrow 0^+} \omega(s, t) = \frac{\pi}{2}, \quad \text{uniformly for } s \text{ in any compact interval } J \subset (0, \infty), \tag{17}$$

$$\lim_{s \rightarrow 0^+} \omega(s, t) = \omega_0^t, \quad \text{uniformly for } t \text{ in any compact interval } J \subset (0, \infty), \tag{18}$$

$$\lim_{t \rightarrow +\infty} t\omega(s_0, t) = \frac{\pi}{2\sqrt{s_0}}, \quad \lim_{s \rightarrow +\infty} \sqrt{s}\omega(s, t_0) = \frac{\pi}{2t_0}, \quad \text{for any fixed } s_0, t_0 > 0. \tag{19}$$

Proof As for (17), given let $\omega_s : (0, \infty) \rightarrow \left(0, \frac{\pi}{2}\right)$ be defined by $\omega_s(t) = \omega(s, t)$. By the Implicit Function Theorem, one has

$$\frac{\partial \omega_s}{\partial t}(t) = - \frac{s\omega(1 + \cotan(\sqrt{st}\omega)^2)}{st(1 + \cotan(\sqrt{st}\omega)^2) + (1 + \tan(\omega)^2)} \Big|_{\omega=\omega_s(t)}$$

and hence $\frac{\partial \omega_s}{\partial t}(t) < 0$ for every t . Consequently, for any fixed $s > 0$ the limit in (17) exists and belongs to $[0, \pi/2]$; moreover, taken $J \subset (0, \infty)$, such a limit is uniform with respect to $s \in J$ as a consequence of the Dini Theorem on the uniform convergence of monotone functions. Fixed $s = s_0 > 0$, we now let $\bar{\omega}_0 = \lim_{t \rightarrow 0^+} \omega(s_0, t) \in \left[0, \frac{\pi}{2}\right]$ and we observe that, from (15), we have

$$\tan(\omega(s_0, t)) \tan(\sqrt{s_0}t\omega(s_0, t)) = \sqrt{s_0} \quad \text{for every } t > 0, \tag{20}$$

which for $t \rightarrow 0^+$ can hold if and only if $\bar{\omega}_0 = \frac{\pi}{2}$, since the second factor of the above left-hand side converges to 0. This proves (18).

Concerning (17), given $t > 0$ we define $\omega_t : (0, \infty) \rightarrow \left(0, \frac{\pi}{2}\right)$ by $\omega_t(s) = \omega(s, t)$ and, again by the Implicit Function Theorem, we have

$$\frac{\partial \omega_t}{\partial s}(s) = \frac{1 - \frac{t\omega \tan(\omega)}{\cos^2(\sqrt{st}\omega)}}{2st \tan(\omega)(1 + \tan(\sqrt{st}\omega)^2) + 2\sqrt{s}(1 + \tan(\omega)^2) \tan(\sqrt{st}\omega)} \Big|_{\omega=\omega_t(s)}.$$

After having observed that the denominator in the above expression is the sum of two positive quantities in view of (16), we notice that the numerator is equal to $1 - \frac{2\sqrt{st}\omega(s, t)}{\sin(2\sqrt{st}\omega(s, t))}$, thanks to (15). Since for any $q \in \left(0, \frac{\pi}{2}\right)$ one has $\frac{2q}{\sin(2q)} > 1$,

it follows that ω_t is decreasing and the limit in (18) exists. It is now sufficient to observe that $\frac{\tan(\sqrt{st}\omega(s, t))}{\sqrt{st}\omega(s, t)} \rightarrow 1$ for $s \rightarrow 0^+$, uniformly in $t \in J$ (thanks to the fact that $\omega(s, t) \in \left(0, \frac{\pi}{2}\right)$ for any s, t), in order to conclude the validity of (18) thanks to (15).

Finally, we deal with the two limits in (19). On the one hand, given again $s = s_0 > 0$ we preliminarily observe that $\lim_{t \rightarrow +\infty} \omega(s_0, t) = 0$, due to (16). Since (20) holds for any t , it is now necessary that $\tan(\sqrt{s_0 t}\omega(s_0, t)) \rightarrow +\infty$ for $t \rightarrow +\infty$; being $\omega(s_0, t) \leq \frac{\pi}{2\sqrt{s_0 t}}$ in view of (16), this necessarily provides $\lim_{t \rightarrow +\infty} t\omega(s_0, t) = \frac{\pi}{2\sqrt{s_0}}$. The second limit in (19) can be shown to hold similarly.

In the following, it will also be useful to consider the *minimization* problems

$$\lambda_i^\pm = \lambda_i^\pm(a, M^0) := \min_{p \in P_{\alpha, \beta}^\pm} k_i^\pm(p) \quad \text{and} \quad \lambda_i^0 = \lambda_i^0(a, M^0) := \min_{p \in P_{\alpha, \beta}^0} k_i^0(p), \quad (21)$$

whose solutions will act as *lower bounds* for $k_i^\pm(p)$ and $k_i^0(p)$. Also in this case it is possible to determine explicitly the exact values of such minima, as stated below.

Proposition 3.4 ([7, Theorem 5]). *For every $i \in \mathbb{N}_+$, it holds*

$$\lambda_i^\pm(a, M^0) = \frac{4i^2}{\beta[2b\pi]^2} \omega^2\left(\frac{\alpha}{\beta}, \frac{1-a-2b}{2b}\right) \quad \text{and} \quad \lambda_i^0(a, M^0) = \frac{i^2}{\beta((a-c)\pi)^2} \omega^2\left(\frac{\alpha}{\beta}, \frac{c}{a-c}\right). \quad (22)$$

where $\omega(\cdot, \cdot)$ is defined by (15).

Notice that each of the values in (22) is attained in correspondence of a unique minimizer, which is constructed by switching the roles of α and β in the previous discussion, accordingly modifying a , b and c ; since our main focus is here on the maximization of the eigenvalues, we refer the interested reader to [7] (pp. 177–178). Whenever needed (in particular, in Remark 3.6 and Remark 4.5), we will denote the unique density achieving the former (resp., the latter) minimum in (21) as $\underline{p}_{i, \pm}$ (resp., $\underline{p}_{i, 0}$).

Summing up, if $0 < \alpha < 1 < \beta$ and $(a, M^0) \in \Omega_{\alpha, \beta}$, for all $p \in \bar{P}_{\alpha, \beta}$ and $i \in \mathbb{N}_+$ the following sharp bounds hold:

$$\lambda_i^\pm(a, M^0) \leq k_i^\pm(p|_{I^\pm}) \leq \Lambda_i^\pm(a, M^0) \quad \text{and} \quad \lambda_i^0(a, M^0) \leq k_i^0(p|_{I^0}) \leq \Lambda_i^0(a, M^0). \quad (23)$$

In the case $M^0 = a$, discussed in Section 4, it is possible to visualize quite neatly how the curves originating from these bounds interlace in the (a, k) -plane (cf. Fig. 6). We remark that, in view of the uniqueness of maximizers (and minimizers) shown in [7], the equality between the upper and the lower bounds in (23) may occur only if $p_i^\pm = \underline{p}_{i, \pm} = \alpha$ or $p_i^\pm = \underline{p}_{i, \pm} = \beta$ a.e. in I^\pm , and similarly in I^0 . In our setting, these cases are ruled out by the strict inequalities in the definition of $\Omega_{\alpha, \beta}$ given in (5).

3.2 Maximizing the first torsional eigenvalue

In this subsection, we focus on the maximization problem

$$\Lambda_1 = \Lambda_1(a, M^0) := \max_{p \in \overline{P}_{\alpha, \beta}} k_1(p). \tag{24}$$

An explicit characterization of the maximizer is given in the following theorem (the reader can also make reference to Figs. 3 and 4 for some visual hints).

Theorem 3.5 *Let $0 < \alpha < 1 < \beta$ and $(a, M^0) \in \Omega_{\alpha, \beta}$. Then, it holds*

$$\Lambda_1 = \Lambda_1(a, M^0) = \min\{\Lambda_1^\pm, \Lambda_1^0\}, \tag{25}$$

where $\Lambda_1^\pm, \Lambda_1^0$ are as in (14). Furthermore, the maximum in (24) is achieved by

$$p^*(x) = \begin{cases} p_1^+(x) & \text{for } x \in I^+ \\ p_1^0(x) & \text{for } x \in I^0 \\ p_1^-(x) & \text{for } x \in I^-, \end{cases} \tag{26}$$

where the functions p_1^\pm and p_1^0 are defined as in (10). More precisely, the following three cases may occur:

- (i) if (a, M^0) is such that $\Lambda_1^\pm = \Lambda_1^0$, then p^* is the unique maximizer for (24);
- (ii) if (a, M^0) is such that $\Lambda_1^\pm < \Lambda_1^0$ and $\bar{p} \in \overline{P}_{\alpha, \beta}$ is a maximizer for (24), then $\bar{p} = p^* = p_1^\pm$ a.e. in I^\pm ;
- (iii) if (a, M^0) is such that $\Lambda_1^\pm > \Lambda_1^0$ and $\bar{p} \in \overline{P}_{\alpha, \beta}$ is a maximizer for (24), then $\bar{p} = p^* = p_1^0$ a.e. in I^0 .

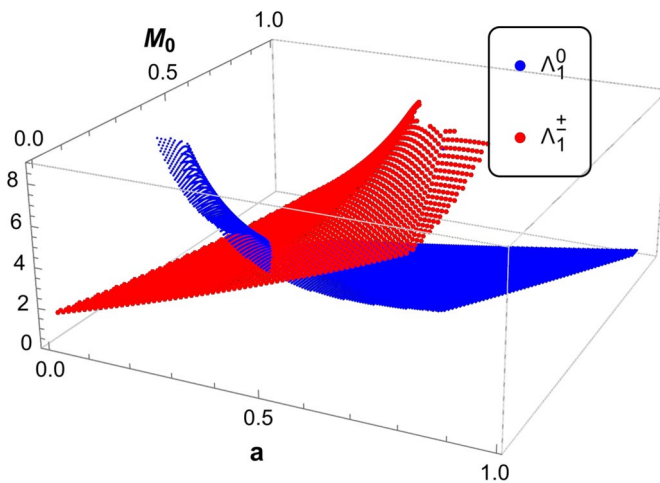


Fig. 4 Plots of the maps $(a, M^0) \in \Omega_{\alpha, \beta} \mapsto \Lambda_1^\pm(a, M^0)$ and $(a, M^0) \in \Omega_{\alpha, \beta} \mapsto \Lambda_1^0(a, M^0)$ for $\alpha = \frac{1}{2}, \beta = \frac{3}{2}$

Proof Let $\bar{p} \in \bar{P}_{\alpha,\beta}$ be a maximizer for (24), namely $\Lambda_1 = k_1(\bar{p})$. By Theorem 2.3, we have

$$\Lambda_1 = \min\{k_1^\pm(\bar{p}|_{I^\pm}), k_1^0(\bar{p}|_{I^0})\}$$

and since $\bar{p}|_{I^\pm} \in P_{\alpha,\beta}^\pm$ and $\bar{p}|_{I^0} \in P_{\alpha,\beta}^0$, we infer that

$$\Lambda_1 \leq \min\{\Lambda_1^\pm, \Lambda_1^0\}.$$

On the other hand, let p^* be as in (26). Then, thanks to (7) and (8), we have that $p^* \in \bar{P}_{\alpha,\beta}$, implying $k_1(p^*) \leq \Lambda_1$. Thanks to Proposition 3.2, moreover, we have that $k_1^\pm(p_1^\pm) = \Lambda_1^\pm$ and $k_1^0(p_1^0) = \Lambda_1^0$. Therefore, by Theorem 2.3, $k_1(p^*) = \min\{\Lambda_1^\pm, \Lambda_1^0\}$ and hence $\min\{\Lambda_1^\pm, \Lambda_1^0\} \leq \Lambda_1$, so that (25) follows. Moreover, p^* achieves the maximum in (24).

For what concerns the uniqueness of the maximizer, we distinguish three cases:

- (i) if $\Lambda_1^\pm = \Lambda_1^0$, then by (25) it holds $\Lambda_1 = \Lambda_1^\pm = \Lambda_1^0$. Hence, if $\bar{p} \in \bar{P}_{\alpha,\beta}$ is a maximizer for (24), it follows that $\bar{p}|_{I^\pm} \in P_{\alpha,\beta}^\pm$ is a maximizer for (13)₁ and $\bar{p}|_{I^0} \in P_{\alpha,\beta}^0$ is a maximizer for (13)₂. Consequently, the uniqueness of the maximizer for both (13)₁ and (13)₂ allows one to infer that $\bar{p}|_{I^\pm} = p_1^\pm$ a.e. in I^\pm and $\bar{p}|_{I^0} = p_1^0$ a.e. in I^0 , so that $\bar{p} = p^*$ a.e. in I ;
- (ii) if $\Lambda_1^\pm < \Lambda_1^0$, then by (25) one has $\Lambda_1 = \Lambda_1^\pm$. Reasoning similarly as before, if $\bar{p} \in \bar{P}_{\alpha,\beta}$ is a maximizer for (24) then $\bar{p}|_{I^\pm}$ is a maximizer for (13)₁, so that $\bar{p}|_{I^\pm} = p_1^\pm$ a.e. in I^\pm by the uniqueness of the maximizer for (13)₁;
- (iii) if $\Lambda_1^\pm > \Lambda_1^0$, then by (25) it follows $\Lambda_1 = \Lambda_1^0$ and it suffices to reason as in case (ii), replacing $^\pm$ with 0 , to infer that $\bar{p}|_{I^0} = p_1^0$ a.e. in I^0 . \square

We underline that the graph of the maximizer p^* defined in (26) is precisely the overall one appearing in the left picture of Fig. 3.

Remark 3.6 We point out that in the above cases (ii) and (iii) the uniqueness of the maximizer for (24) may fail. We provide an explicit example in this respect for case (ii) (a similar argument works for case (iii)). Consider the function $p^\dagger \in \bar{P}_{\alpha,\beta}$ defined by

$$p^\dagger(x) = \begin{cases} p_1^+(x) & \text{for } x \in I^+ \\ p_{1,0}^-(x) & \text{for } x \in I^0 \\ p_1^-(x) & \text{for } x \in I^- \end{cases},$$

where p_1^\pm is as in (10), while $p_{1,0}^- \in P_{\alpha,\beta}^0$ is the density achieving the minimum λ_1^0 in (21).

If a and M^0 are chosen in such a way that $\Lambda_1^0(a, M^0) > \lambda_1^0(a, M^0) > \Lambda_1^\pm(a, M^0)$ (a case that occurs, e.g., when $a = M^0$ and a is sufficiently small: take $a < a_1^\pm$ in the left picture of Fig. 6), then Theorem 2.3 yields $k_1(p^\dagger) = \min\{\Lambda_1^\pm, \lambda_1^0\} = \Lambda_1^\pm$. On the other hand, for this choice of a and M^0 , it follows from (25) that $\Lambda_1 = \Lambda_1^\pm$, whence p^\dagger

is a maximizer for (24). Since $p^\dagger \neq p^*$ (recall that $p_1^0 \neq \underline{p}_{1,0}$ for $(a, M^0) \in \Omega_{\alpha,\beta}$), this provides an example where the uniqueness fails. Other maximizers may be defined by modifying the definition of p^\dagger in I^0 in such a way that the inequality $k_1^0(p^\dagger|_{I^0}) > \Lambda_1^\pm$ is preserved.

3.3 Maximizing the Second Torsional Eigenvalue

By Theorem 2.3, the second torsional eigenvalue of (3) is given by

$$k_2(p) = \min_{1 \leq j \leq 2} \{ \{k_j^\pm(p|_{I^\pm}), k_j^0(p|_{I_0})\} / \min\{k_1^\pm(p|_{I^\pm}), k_1^0(p|_{I_0})\} \}. \tag{27}$$

In this subsection, we consider the problem

$$\Lambda_2 = \Lambda_2(a, M^0) := \max_{p \in \bar{P}_{\alpha,\beta}} k_2(p). \tag{28}$$

We have already seen in Remark 3.6 how the order of the (Dirichlet) eigenvalues of the problems in (4) is crucial to compute the maximum value and to characterize the maximizer(s). In this respect, we set the following notation:

$$\Omega_{\alpha,\beta}^0 := \{(a, M^0) \in \Omega_{\alpha,\beta} : k_1^\pm(p|_{I^\pm}) > k_1^0(p|_{I_0}) \text{ for all } p \in \bar{P}_{\alpha,\beta}\}$$

$$\Omega_{\alpha,\beta}^\pm := \{(a, M^0) \in \Omega_{\alpha,\beta} : k_1^\pm(p|_{I^\pm}) < k_1^0(p|_{I_0}) \text{ for all } p \in \bar{P}_{\alpha,\beta}\}$$

$$\Omega_{\alpha,\beta}^\pm := \{(a, M^0) \in \Omega_{\alpha,\beta} : k_1^\pm(p|_{I^\pm}) = k_1^0(p|_{I_0}) \text{ for some } p \in \bar{P}_{\alpha,\beta}\}.$$

The above sets are all nonempty (as can easily be seen, e.g., in the case $M^0 = a$, see Theorem 4.1 and Remark 4.5); we first show that they form a partition of $\Omega_{\alpha,\beta}$.

Proposition 3.7 *Let $0 < \alpha < 1 < \beta$. It holds $\Omega_{\alpha,\beta} = \Omega_{\alpha,\beta}^0 \cup \Omega_{\alpha,\beta}^\pm \cup \Omega_{\alpha,\beta}^\pm$.*

Proof Obviously, $\Omega_{\alpha,\beta}^0$, $\Omega_{\alpha,\beta}^\pm$ and $\Omega_{\alpha,\beta}^\pm$ are pairwise disjoint. Let $(a, M^0) \notin (\Omega_{\alpha,\beta}^\pm \cup \Omega_{\alpha,\beta}^0)$: then, there exist two densities $q, q' \in \bar{P}_{\alpha,\beta}$ such that

$$k_1^\pm(q|_{I^\pm}) \leq k_1^0(q|_{I_0}), \quad k_1^\pm(q'|_{I^\pm}) \geq k_1^0(q'|_{I_0}). \tag{29}$$

If the equality holds in one of the above, then either q or q' realizes the condition in the definition of $\Omega_{\alpha,\beta}^\pm$, yielding $(a, M^0) \in \Omega_{\alpha,\beta}^\pm$. Assume thus that the two inequalities in (29) hold with strict sign. In order to prove that $(a, M^0) \in \Omega_{\alpha,\beta}^0$, we observe that the function

$$\varphi : [0, 1] \rightarrow \mathbb{R}, \quad \varphi(s) := k_1^\pm[(sq + (1-s)q')|_{I^\pm}] - k_1^0[(sq + (1-s)q')|_{I_0}]$$

is continuous by composition: indeed, $s \mapsto sq + (1-s)q'$ is continuous from \mathbb{R} to $\overline{P}_{\alpha,\beta} \subset L^\infty$ (this last endowed with the weak*-topology) thanks to the Lebesgue dominated convergence Theorem, while the fact that $sq + (1-s)q' \mapsto k_1^\pm[(sq + (1-s)q')|_{I^\pm}] - k_1^0[(sq + (1-s)q')|_{I^0}]$ is continuous with respect to the weak* topology follows as recalled in the proof of Proposition 3.1. Since $\varphi(0) > 0$ and $\varphi(1) < 0$ by assumption, by the Intermediate Value Theorem there exists $\bar{s} \in (0, 1)$ for which $\bar{s}q + (1-\bar{s})q'$ realizes the equality in the definition of $\Omega_{\alpha,\beta}^\pm$, proving the statement.

We are now able to state our maximization result for the second torsional eigenvalue.

Theorem 3.8 *Let $0 < \alpha < 1 < \beta$ and $(a, M^0) \in \Omega_{\alpha,\beta}$. Then, $\Lambda_2 \leq \min\{\Lambda_2^\pm, \Lambda_2^0\}$, where $\Lambda_2^\pm, \Lambda_2^0$ are as in (14). Moreover;*

(i) *if $(a, M^0) \in \Omega_{\alpha,\beta}^\pm$, then*

$$\Lambda_1 = \Lambda_1^\pm \quad \text{and} \quad \Lambda_2 = \min\{\Lambda_1^0, \Lambda_2^\pm\} \quad (30)$$

and the maximum in (28) is achieved by

$$\check{p}(x) = \begin{cases} p_2^+(x) & \text{for } x \in I^+ \\ p_1^0(x) & \text{for } x \in I^0 \\ p_2^-(x) & \text{for } x \in I^- \end{cases}, \quad (31)$$

where the functions p_1^0 and p_2^\pm are defined as in (10) and in (11). Furthermore,

- *if (a, M^0) is such that $\Lambda_2 = \Lambda_2^\pm$ and \bar{p}_2 is a maximizer for (28), then $\bar{p}_2 = \check{p}$ a.e. in I^\pm ;*
- *if (a, M^0) is such that $\Lambda_2 = \Lambda_1^0$ and \bar{p}_2 is a maximizer for (28), then $\bar{p}_2 = \check{p}$ a.e. in I^0 .*

(ii) *if $(a, M^0) \in \Omega_{\alpha,\beta}^0$, then*

$$\Lambda_1 = \Lambda_1^0 \quad \text{and} \quad \Lambda_2 = \min\{\Lambda_1^\pm, \Lambda_2^0\} \quad (32)$$

and the maximum in (28) is achieved by

$$\hat{p}(x) = \begin{cases} p_1^+(x) & \text{for } x \in I^+ \\ p_2^0(x) & \text{for } x \in I^0 \\ p_1^-(x) & \text{for } x \in I^- \end{cases}, \quad (33)$$

where the functions p_1^\pm and p_2^0 are defined as in (10) and in (12). Furthermore,

- *if (a, M^0) is such that $\Lambda_2 = \Lambda_1^\pm$ and \bar{p}_2 is a maximizer for (28), then $\bar{p}_2 = \hat{p}$ a.e. in I^\pm ;*

- if (a, M^0) is such that $\Lambda_2 = \Lambda_2^0$, and \bar{p}_2 is a maximizer for (28), then $\bar{p}_2 = \hat{p}$ a.e. in I^0 ;

(iii) if $(a, M^0) \in \Omega_{\alpha,\beta}^-$, then

$$\Lambda_2 \geq \min\{\lambda_2^\pm, \lambda_2^0\}. \tag{34}$$

Proof The fact that $\Lambda_2 \leq \min\{\Lambda_2^\pm, \Lambda_2^0\}$ for every $(a, M^0) \in \Omega_{\alpha,\beta}$ is a direct consequence of (27). Next, we turn to the proof of item (i). Assuming that $(a, M^0) \in \Omega_{\alpha,\beta}^\pm$, for all $p \in \bar{P}_{\alpha,\beta}$ it holds that $k_1(p) = k_1^\pm(p|_{I^\pm})$ and $k_2(p) = \min\{k_1^0(p|_{I^0}), k_2^\pm(p|_{I^\pm})\}$. Hence, $\Lambda_1 = \Lambda_1^\pm$ and $\Lambda_2 = \max_{p \in \bar{P}_{\alpha,\beta}} k_2(p) \leq \min\{\Lambda_1^0, \Lambda_2^\pm\}$. On the other hand, since by construction $\Lambda_1 < \Lambda_2$, we infer that $\Lambda_1 < \Lambda_1^0$. For \check{p} defined as in (31), we then have

$$k_1(\check{p}) = \min\{k_1^\pm(\check{p}|_{I^\pm}), k_1^0(\check{p}|_{I^0})\} = \min\{k_1^\pm(\check{p}|_{I^\pm}), \Lambda_1^0\} = k_1^\pm(\check{p}|_{I^\pm}),$$

where the last equality follows from the fact that $k_1^\pm(\check{p}|_{I^\pm}) \leq \Lambda_1 < \Lambda_1^0$. Then,

$$k_2(\check{p}) = \min\{k_1^0(\check{p}|_{I^0}), k_2^\pm(\check{p}|_{I^\pm})\} = \min\{\Lambda_1^0, \Lambda_2^\pm\}.$$

This shows that $\min\{\Lambda_1^0, \Lambda_2^\pm\} \leq \Lambda_2$ and hence (30) holds, whence (i) is proved.

Concerning the proof of (ii), if $(a, M^0) \in \Omega_{\alpha,\beta}^0$ then $k_1(p) = k_1^0(p|_{I^0})$ and $k_2(p) = \min\{k_1^\pm(p|_{I^\pm}), k_2^0(p|_{I^0})\}$. One can then obtain (32) and prove (ii) thanks to arguments similar to the ones for case (i), exchanging the superscripts 0 and $^\pm$.

Finally, for the proof of (iii), if $(a, M^0) \in \Omega_{\alpha,\beta}^-$ then $k_1^\pm(p|_{I^\pm}) = k_1^0(p|_{I^0})$ for some $p \in \bar{P}_{\alpha,\beta}$ and

$$k_2(p) = \min\{k_2^\pm(p|_{I^\pm}), k_2^0(p|_{I^0})\}.$$

Therefore, (34) readily follows.

In Fig. 5, with the same positions as for Fig. 3, we depict the graphs of the densities in (33) (left picture) and (31) (right picture).

As for case (iii), we remark that if $(a, M^0) \in \Omega_{\alpha,\beta}^-$ then the first eigenvalue can be triple and there is no clear correspondence between the second eigenvalue of (3) and those of the associated Dirichlet problems. This is the reason why we only have the lower bound (34). In the other cases, Theorem 3.8 provides a rather complete characterization of Λ_2 , although the sets $\Omega_{\alpha,\beta}^0$ and $\Omega_{\alpha,\beta}^\pm$ are generally defined in an implicit way.

In the next section, we focus on the case $M^0 = a$, where it is possible to visualize quite neatly the picture for the eigenvalues of (3) and, in turn, to determine the above mentioned sets more explicitly.

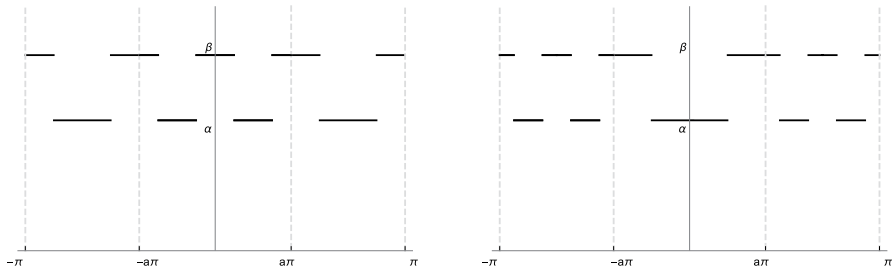


Fig. 5 Graphs of the maximizers introduced in Theorem 3.8

4 The Case $M^0 = a$

The case $M^0 = a$ corresponds to requiring that the total mass distributed on the central span exactly corresponds to its length; such a choice is always admissible in our framework, namely $(a, a) \in \Omega_{\alpha, \beta}$ for any $0 < a < 1$. In this case, the bounds (23) regarding the eigenvalues of (3) become much more readable. Precisely, since

$$b = \frac{(1 - a)(1 - \alpha)}{2(\beta - \alpha)}, \quad c = \frac{(\beta - 1)a}{\beta - \alpha},$$

setting

$$\gamma := \frac{(\beta - \alpha)^2}{\alpha[(\beta - 1)\pi]^2} \omega^2 \left(\frac{\beta}{\alpha}, \frac{1 - \alpha}{\beta - 1} \right) \quad \text{and} \quad \delta := \frac{(\beta - \alpha)^2}{\beta[(1 - \alpha)\pi]^2} \omega^2 \left(\frac{\alpha}{\beta}, \frac{\beta - 1}{1 - \alpha} \right) \tag{35}$$

one immediately has, for every $0 < a < 1$, that

$$\begin{aligned} \lambda_i^\pm(a) &:= \lambda_i^\pm(a, a) = \frac{4i^2\delta}{(1 - a)^2}, & \lambda_i^0(a) &:= \lambda_i^0(a, a) = \frac{i^2\delta}{a^2} \\ \Lambda_i^\pm(a) &:= \Lambda_i^\pm(a, a) = \frac{4i^2\gamma}{(1 - a)^2}, & \Lambda_i^0(a) &:= \Lambda_i^0(a, a) = \frac{i^2\gamma}{a^2}. \end{aligned} \tag{36}$$

We stress that, for every $i \in \mathbb{N}_+$, the functions $a \mapsto \lambda_i^\pm(a), \Lambda_i^\pm(a)$ are monotone increasing, while the functions $a \mapsto \lambda_i^0(a), \Lambda_i^0(a)$ are monotone decreasing, in accord with the usual monotonicity properties of the Dirichlet eigenvalues with respect to the length of the considered interval [6, Section 1.3.2].

It is immediate to draw the graphs of $\lambda_i^\pm, \Lambda_i^\pm, \lambda_i^0, \Lambda_i^0$ in the (a, λ) -plane; recalling that $\lambda_i^\pm \leq k_i^\pm(p) \leq \Lambda_i^\pm$ and $\lambda_i^0 \leq k_i^0(p) \leq \Lambda_i^0$ for every $p \in \bar{P}_{\alpha, \beta}$, such graphs enclose a family of regions of the (a, λ) -plane where the eigenvalues of the Dirichlet problems on the central and on the lateral spans are found (as functions of a), see the left picture in Fig. 6. In particular, we can give conditions on a for which the first N eigenvalues of (3) (for a given positive integer N) all coincide with Dirichlet eigenvalues on the central (or on the lateral) span. To this end, for $N \in \mathbb{N}_+$, we let $0 < a_N^0, a_N^\pm < 1$ be defined by

$$\lambda_1^0(a_N^\pm) = \Lambda_N^\pm(a_N^\pm) \quad \text{and} \quad \lambda_1^\pm(a_N^0) = \Lambda_N^0(a_N^0); \tag{37}$$

explicitly, taking into account (36),

$$a_N^\pm = \frac{\sqrt{\delta}}{\sqrt{\delta} + 2N\sqrt{\gamma}}, \quad a_N^0 = \frac{N\sqrt{\gamma}}{2\sqrt{\delta} + N\sqrt{\gamma}}. \tag{38}$$

For future purposes, notice that $a_N^\pm < \frac{1}{3} < a_N^0 < 1$ for all $N \in \mathbb{N}_+$ (recall that, from (23) and (36), $\delta < \gamma$). The following then holds.

Theorem 4.1 *Let $0 < \alpha < 1 < \beta$ and $M^0 = a$ with $0 < a < 1$. Furthermore, let $N \in \mathbb{N}_+$ be fixed and let $a_N^\pm < a_N^0$ be as in (37). Then, for every $1 \leq i \leq N$ and every $p \in \bar{P}_{\alpha,\beta}$, it holds that*

- (i) *if $0 < a < a_N^\pm$, then $(a, a) \in \Omega_{\alpha,\beta}^\pm$ and $k_i(p) = k_i^\pm(p|_{I^\pm})$;*
- (ii) *if $a_N^0 < a < 1$, then $(a, a) \in \Omega_{\alpha,\beta}^0$ and $k_i(p) = k_i^0(p|_{I^0})$.*

Furthermore, if $a_N^0 < a < 1$ then k_i is simple for every $i = 1, \dots, N$ (with associated eigenfunction being equal to zero on the side spans).

Proof From (23) and (36) - thanks to the previously recalled monotonicity properties of Λ_i^\pm and Λ_i^0 with respect to a , we infer that

$$0 < a < a_N^\pm \Rightarrow k_1^\pm(p|_{I^\pm}) < \dots < k_N^\pm(p|_{I^\pm}) \leq \Lambda_N^\pm(a) < \lambda_1^0(a) \leq k_1^0(p|_{I^0}) \quad \text{for all } p \in \bar{P}_{\alpha,\beta},$$

i.e., $(a, a) \in \Omega_{\alpha,\beta}^\pm$, and

$$a_N^0 < a < 1 \Rightarrow k_1^0(p|_{I^0}) < \dots < k_N^0(p|_{I^0}) \leq \Lambda_N^0(a) < \lambda_1^\pm(a) \leq k_1^\pm(p|_{I^\pm}) \quad \text{for all } p \in \bar{P}_{\alpha,\beta},$$

i.e., $(a, a) \in \Omega_{\alpha,\beta}^0$. The statement then follows by combining the above inequalities with the statement of Theorem 2.3.

We thus observe that, the larger is a , the more relevant the central span is, since the first eigenvalues of (3) coincide with the Dirichlet eigenvalues on the central span in larger number, while the opposite occurs as long as a gets closer to 0.

Remark 4.2 In view of Theorem 2.3, the knowledge of the intersection points between the graphs of the functions defined in (36) is important in order to provide explicit estimates for the eigenvalues of (3). From (36), we then infer

$$\Lambda_i^\pm(a) = \Lambda_i^0(a) \iff a = \frac{1}{3} \iff \lambda_i^\pm(a) = \lambda_i^0(a) \quad \text{for every } i \in \mathbb{N}_+ \tag{39}$$

and, similarly,

$$\Lambda_i^\pm(a) = \Lambda_{i+1}^0(a) \iff a = \frac{i+1}{3i+1} \iff \lambda_i^\pm(a) = \lambda_{i+1}^0(a) \quad \text{for every } i \in \mathbb{N}_+$$

and

$$\Lambda_{i+1}^\pm(a) = \Lambda_i^0(a) \iff a = \frac{i}{3i+2} \iff \lambda_{i+1}^\pm(a) = \lambda_i^0(a) \text{ for every } i \in \mathbb{N}_+.$$

Specifically, we have $\Lambda_1^\pm(a) = \Lambda_2^0(a)$ if and only if $a = \frac{1}{2}$ and $\Lambda_2^\pm(a) = \Lambda_1^0(a)$ if and only if $a = \frac{1}{5}$.

4.1 Maximizing the Torsional Eigenvalues in the Case $M^0 = a$.

As for the maximization of the torsional eigenvalues under the assumption $M^0 = a$, we first observe that Theorem 3.5, thanks to (39), yields the following corollary which provides an explicit characterization of the maximizer for the *first* eigenvalue in dependence on a (see the right picture in Fig. 6).

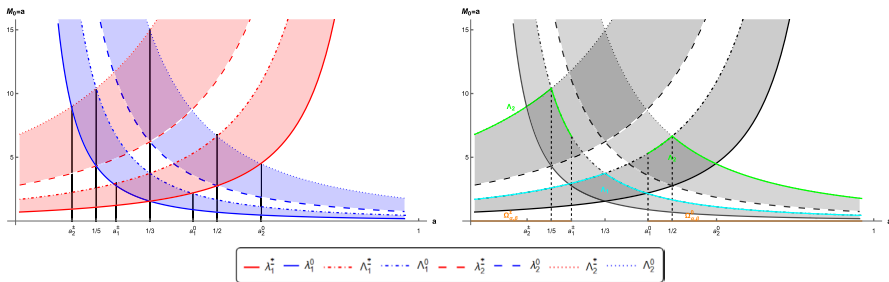


Fig. 6 Plots of the curves $a \mapsto \lambda_i^\pm(a)$, $a \mapsto \Lambda_i^\pm(a)$, $a \mapsto \lambda_i^0(a)$ and $a \mapsto \Lambda_i^0(a)$ for $i = 1, 2$ and $M^0 = a$ fixed, $\alpha = \frac{1}{2}$, $\beta = 2$ (left) and of the curves $a \mapsto \Lambda_1(a)$ and $a \mapsto \Lambda_2(a)$ (right)

Corollary 4.3 *Let $0 < \alpha < 1 < \beta$ and $M^0 = a$ with $0 < a < 1$. Moreover, let γ and p^* as in (35) and (26), respectively. Then, the maximum Λ_1 in (24) and the corresponding maximizer \bar{p} are characterized as follows:*

- (i) if $a = \frac{1}{3}$, then $\Lambda_1\left(\frac{1}{3}\right) = \Lambda_1^\pm\left(\frac{1}{3}\right) = \Lambda_1^0\left(\frac{1}{3}\right) = 9\gamma$ and $\bar{p} = p^*$;
- (ii) if $a < \frac{1}{3}$, then $\Lambda_1(a) = \Lambda_1^\pm(a) = \frac{4\gamma}{(1-a)^2}$ and $\bar{p} = p^*$ a.e. in I^\pm ;
- (iii) if $a > \frac{1}{3}$, then $\Lambda_1(a) = \Lambda_1^0(a) = \frac{\gamma}{a^2}$ and $\bar{p} = p^*$ a.e. in I^0 .

Furthermore, the assumption $M^0 = a$ allows us to complete the statement of Theorem 3.8 with more precise information also about the *second* eigenvalue, as follows (see again the right picture in Fig. 6).

Corollary 4.4 *Let $0 < \alpha < 1 < \beta$ and $M^0 = a$ with $0 < a < 1$. Furthermore, let a_1^\pm, a_1^0 as in (38) (with $N = 1$) and \check{p}, \hat{p} as in (31) and (33), respectively. Then, the following hold:*

- (i) *if $0 < a < a_1^\pm$, then $\Lambda_2(a) = \min\{\Lambda_1^0(a), \Lambda_2^\pm(a)\}$ and the maximum in (28) is achieved by the function \check{p} . Moreover,*

$$\Lambda_2(a) = \begin{cases} \frac{16\gamma}{(1-a)^2} & \text{if } 0 < a < \min\{\frac{1}{5}, a_1^\pm\} \\ \frac{\gamma}{a^2} & \text{if } \frac{1}{5} \leq a < a_1^\pm \end{cases} \tag{40}$$

so that, for all $0 < \varepsilon < a_1^\pm$,

$$\max_{0 < a \leq a_1^\pm - \varepsilon} \Lambda_2(a) = \begin{cases} \frac{16\gamma}{(1+\varepsilon-a_1^\pm)^2} & \text{if } a_1^\pm < \frac{1}{5} \\ 25\gamma & \text{if } \frac{1}{5} \leq a_1^\pm; \end{cases}$$

- (ii) *if $a_1^0 < a < 1$, then $\Lambda_2(a) = \min\{\Lambda_1^\pm(a), \Lambda_2^0(a)\}$ and the maximum in (28) is achieved by the function \hat{p} . Moreover,*

$$\Lambda_2(a) = \begin{cases} \frac{4\gamma}{(1-a)^2} & \text{if } a_1^0 < a \leq \frac{1}{2} \\ \frac{4\gamma}{a^2} & \text{if } \max\{\frac{1}{2}, a_1^0\} < a < 1, \end{cases} \tag{41}$$

so that, for all $0 < \varepsilon < 1 - a_1^0$,

$$\max_{a_1^0 + \varepsilon \leq a < 1} \Lambda_2(a) = \begin{cases} 16\gamma & \text{if } a_1^0 \leq \frac{1}{2} \\ \frac{4\gamma}{(a_1^0 + \varepsilon)^2} & \text{if } \frac{1}{2} < a_1^0 < 1. \end{cases}$$

Proof Using Theorem 4.1, if $0 < a < a_1^\pm$ (resp., $a_1^0 < a < 1$), then $(a, a) \in \Omega_{\alpha, \beta}^\pm$ (resp., $(a, a) \in \Omega_{\alpha, \beta}^0$). Therefore, the statement follows from Theorem 3.8, observing that (40) and (41) follow from the explicit bounds (36) and directly provide the value of $\max_a \Lambda_2(a)$.

Remark 4.5 **The “extremal” cases $a = a_1^\pm$ and $a = a_1^0$.** These cases are excluded from the statement of Corollary 4.4 since $(a_1^\pm, a_1^\pm), (a_1^0, a_1^0) \in \Omega_{\alpha, \beta}^\pm$, and hence Theorem 3.8 does not allow one to conclude the exact value of $\Lambda_2(a)$. To see this, consider the two densities

$$p_\pm^\pm(x) = \begin{cases} p_1^+(x) & \text{for } x \in I^+ \\ p_{1,0}^\pm(x) & \text{for } x \in I^0 \\ p_1^-(x) & \text{for } x \in I^- \end{cases} \quad \text{and} \quad p_\pm^0(x) = \begin{cases} p_{1,+}^0(x) & \text{for } x \in I^+ \\ p_1^0(x) & \text{for } x \in I^0 \\ p_{1,-}^0(x) & \text{for } x \in I^- \end{cases}$$

where, with the previous notation, $p_{1,\pm}, p_{1,0}, p_1^\pm$ achieve, respectively, $\lambda_1^\pm(a_1^\pm), \lambda_1^0(a_1^0), \Lambda_1^\pm(a_1^\pm)$. Recalling the first formula in (37) (with $N = 1$), it holds that

$$k_1^\pm(p_\pm^\pm|_{I^\pm}) = \Lambda_1^\pm(a_1^\pm) = \lambda_1^0(a_1^\pm) = k_1^0(p_\pm^\pm|_{I^0}). \tag{42}$$

Consequently, $(a_1^\pm, a_1^\pm) \in \Omega_{\alpha,\beta}^\pm$. Similarly, by reasoning on the density p_\pm^0 , we get $(a_1^0, a_1^0) \in \Omega_{\alpha,\beta}^\pm$.

The above observation suggests that one may try to extend the statement of Corollary 4.4 to the cases $a = a_1^\pm$ and $a = a_1^0$ provided that the densities p_\pm^\pm and p_\pm^0 , respectively, are excluded. In fact, if $a = a_1^\pm$, recalling (42) we have

$$k_1^\pm(q|_{I^\pm}) \leq k_1^\pm(p_\pm^\pm|_{I^\pm}) = \Lambda_1^\pm(a_1^\pm) = \lambda_1^0(a_1^\pm) = k_1^0(p_\pm^\pm|_{I^0}) \leq k_1^0(q|_{I^0}) \quad \text{for any } q \in \bar{P}_{\alpha,\beta}; \tag{43}$$

if $q \in \bar{P}_{\alpha,\beta} \setminus \{p_\pm^\pm\}$, by the uniqueness of both minimizer and maximizer for the Dirichlet problems on each span (cf. Proposition 3.2), at least one of the two inequalities in (43) is then strict. Therefore, $(a_1^\pm, a_1^\pm) \in \Omega_{\alpha,\beta}^\pm$ as long as we replace $\bar{P}_{\alpha,\beta}$ with $\bar{P}_{\alpha,\beta} \setminus \{p_\pm^\pm\}$. As a consequence, item (i) in Theorem 3.8 yields $\Lambda_2 = \min\{\Lambda_1^0, \Lambda_2^\pm\}$ and the maximum in (28) (having excluded $p = p_\pm^\pm$) is achieved by the function \check{p} . Therefore, if this extra condition is assumed, item (i) of Corollary 4.4 holds up to $a = a_1^\pm$ and

$$\max_{0 < a \leq a_1^\pm} \Lambda_2(a) = \begin{cases} \Lambda_2(a_1^\pm) & \text{if } a_1^\pm < \frac{1}{5} \\ \Lambda_2\left(\frac{1}{5}\right) & \text{if } \frac{1}{5} \leq a_1^\pm. \end{cases}$$

A similar argument can be invoked if $a = a_1^0$ and $p \neq p_\pm^0$.

Remark 4.6 The values a_1^\pm and a_1^0 . By direct computation, it can be easily seen that the inequalities and $a_1^0 \leq \frac{1}{2}$ are both equivalent to the requirement that

$$\sqrt{\gamma} \leq 2\sqrt{\delta}. \tag{44}$$

Such an inequality holds in several different situations. To see this, observe first that, fixed $\beta > 1$ (resp., $\alpha < 1$), it can be directly checked that $\gamma \rightarrow \frac{1}{4}$ (resp., $\delta \rightarrow \frac{1}{4}$) for $\alpha \rightarrow 1^-$ (resp., $\beta \rightarrow 1^+$), as a consequence of (17). On the other hand, a direct computation shows that for given $\varsigma > 0$, setting $g(t) = 1 - \frac{1}{t}$ also $h(t) := \omega(sg(t), \varsigma t)$ has a limit for $t \rightarrow +\infty$, since h is monotone decreasing for large t . Indeed,

$$h'(t) = \frac{g'(t) \left(\frac{\text{scotan}(\sqrt{sg(t)\varsigma t\omega})}{2\sqrt{sg(t)}} - \frac{\varsigma t\omega(1 + \text{cotan}^2(\sqrt{sg(t)\varsigma t\omega}))}{2} \right) - \varsigma sg(t)(1 + \text{cotan}^2(\sqrt{sg(t)\varsigma t\omega}))}{sg(t)\varsigma t(1 + \text{cotan}(\sqrt{sg(t)\varsigma t\omega})^2)(1 + \tan^2 \omega)}$$

< 0 for $t \rightarrow +\infty$,

as can be seen by replacing the explicit expression of g . Hence, in view of (16), $h(t) \rightarrow 0$ for $t \rightarrow +\infty$. Similarly as for (19), for fixed $s > 0$ and every t it has now to be

$$\tan(\omega(sg(t), \varsigma t)) \tan(\sqrt{sg(t)\varsigma}t\omega(sg(t), \varsigma t)) = \sqrt{sg(t)},$$

hence necessarily $t\omega(sg(t), \varsigma t) \rightarrow \frac{\pi}{2\varsigma\sqrt{s}}$. Setting $s = \frac{1}{\beta}$, $\varsigma = \beta - 1$ and $t = \frac{1}{1 - \alpha}$ we finally obtain $\delta \rightarrow \frac{1}{4}$ for $\alpha \rightarrow 1^-$. In the same way, it can be seen that $\gamma \rightarrow \frac{1}{4}$ for $\beta \rightarrow 1^+$. This means that (44) holds both for $\alpha \rightarrow 1^-$ (if β is fixed) and for $\beta \rightarrow 1^+$ (if α is fixed).

Even more, if $\alpha = 1 - \zeta$ and $\beta = 1 + \zeta$ for $\zeta \in (0, 1)$, then (44) is automatically true. Indeed, writing the explicit expressions of γ and δ in this case, it turns out that

$$\sqrt{\gamma} = \rho(\zeta)\sqrt{\delta}, \quad \text{with} \quad \rho(\zeta) = \sqrt{\frac{1 + \zeta}{1 - \zeta} \frac{\omega\left(\frac{1 + \zeta}{1 - \zeta}, 1\right)}{\omega\left(\frac{1 - \zeta}{1 + \zeta}, 1\right)}} \leq \frac{4}{\pi} \sqrt{\frac{1 + \zeta}{1 - \zeta}} \omega\left(\frac{1 + \zeta}{1 - \zeta}, 1\right),$$

where we have exploited the equality $\omega(1, 1) = \pi/4$ together with the fact that $s \mapsto \omega(s, t)$ is decreasing, as shown in the proof of Proposition 3.3. Since $s \mapsto \sqrt{s}\omega(s, 1) = \arctan\left(\frac{\sqrt{s}}{\tan(\omega(s, 1))}\right)$ is an increasing function, as one can check by computing the derivative of the right-hand side with respect to s , we finally infer that $\rho(\zeta) \leq \frac{4}{\pi} \frac{\pi}{2} = 2$, thanks to the second limit in (19). Incidentally, notice that in fact $\rho(\zeta) \rightarrow 1$ for $\zeta \rightarrow 0$ (by continuity) and $\rho(\zeta) \rightarrow \frac{\pi}{2\omega_0^1} < 2$ for $\zeta \rightarrow 1$ (here $\omega_0^1 \approx 0.86$ denotes the solution of $\omega_0^1 \tan(\omega_0^1) = 1$), thanks to (18) with $t = 1$.

A situation where (44) fails can instead be obtained considering $\alpha = 1/\beta$: in this case, one has $\frac{1 - \alpha}{\beta - 1} = \frac{1}{\beta}$ and, using the definition of ω in (15),

$$\sqrt{\gamma} = \frac{\omega\left(\beta^2, \frac{1}{\beta}\right)}{\omega\left(\frac{1}{\beta^2}, \beta\right)} \sqrt{\delta} = \frac{\arctan \sqrt{\beta}}{\arctan \frac{1}{\sqrt{\beta}}} \sqrt{\delta}. \tag{45}$$

Therefore, it turns out that $\beta^* = 3$ plays the role of a “critical” value, since the coefficient in front of $\sqrt{\delta}$ is larger than 2, making (44) fail, if and only if $\beta > \beta^*$. Incidentally, notice that the case $\beta = 3$, $\alpha = 1/3$ was dealt with in [5] as a “limit” situation from an applied point of view, since the heavier material has a density which is 9 times the one of the lighter material, fact that could look quite uncommon in engineering. We also mention that (45) allows one to clearly see that $\gamma > \delta$, in accord with the estimates in [7], since $\beta > 1$ by assumption.

Summarizing, in view of the above evidence we have that

(44) fails as long as the two densities α and β are sufficiently unbalanced.

In Fig. 7, we report another instance of this fact, for $\beta = 4$ and $\alpha = 0.35$, namely two unbalanced densities (here $\sqrt{\gamma} \approx 0.798$ and $2\sqrt{\delta} \approx 0.759$). The figure displays only the plots of the bounds for the eigenvalues needed to determine a_i^\pm and a_i^0 ($i = 1, 2$) and shows that, in this case, $a_1^\pm < \frac{1}{5}$ and $a_1^0 > \frac{1}{2}$.

Remark 4.7 Optimality and physical interpretation of Corollary 4.4. It is known from [27] that the “physical range” for a , namely the choice of the position of the piers corresponding to the configuration of the majority of real bridges, is

$$\frac{1}{2} \leq a \leq \frac{2}{3}.$$

If $M^0 = a$ and $a_1^0 \leq \frac{1}{2}$ (recall the discussion in Remark 4.6), Corollary 4.3 and Corollary 4.4 give a complete scenario in this range. Indeed, we have

$$\max_{\frac{1}{2} \leq a < 1} \Lambda_1(a) = \Lambda_1\left(\frac{1}{2}\right) = \Lambda_1^0\left(\frac{1}{2}\right) = 4\gamma \quad \text{and} \quad \max_{\frac{1}{2} \leq a < 1} \Lambda_2(a) = \Lambda_2\left(\frac{1}{2}\right) = \Lambda_2^0\left(\frac{1}{2}\right) = 16\gamma$$

and the two corresponding maximizers are, respectively, the function p^* defined in (26) and the function \hat{p} defined in (33). On the other hand, recalling that at the same time we have $\frac{1}{5} \leq a_1^\pm$ (cf. (44)), the statement of Corollary 4.4 provides $\Lambda_2\left(\frac{1}{5}\right) = 25\gamma > 16\gamma = \Lambda_2\left(\frac{1}{2}\right)$, hence in this case a quite short central span

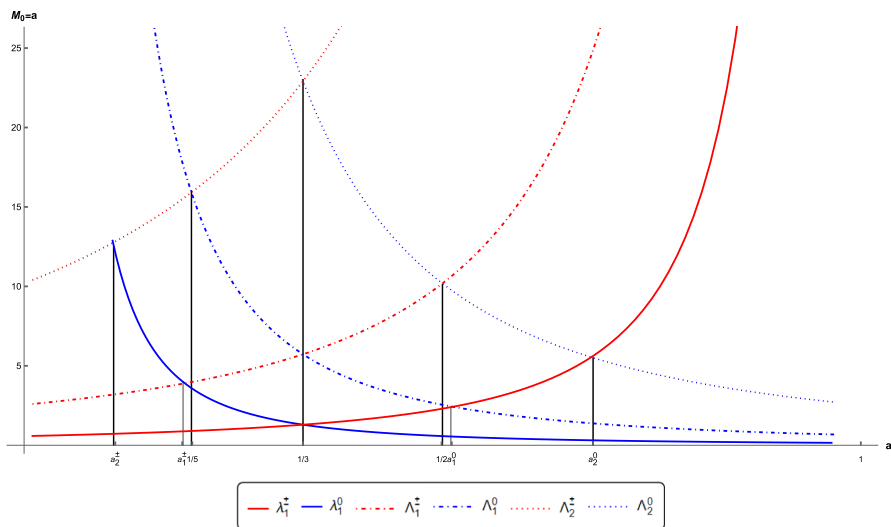


Fig. 7 Plots of the curves $a \mapsto \lambda_i^\pm(a)$, $a \mapsto \Lambda_i^\pm(a)$, $a \mapsto \lambda_i^0(a)$ and $a \mapsto \Lambda_i^0(a)$ for $i = 1, 2$, $M^0 = a$ fixed, $\alpha = 0.35$, $\beta = 4$

would look more advantageous for the maximization of the second torsional eigenvalue. From the point of view of the applications this may seem counterintuitive, but several other factors have to be taken into account. We have seen that the choice $a = \frac{1}{5}$ produces $\Lambda_2 = \Lambda_2^\pm$; in this case, the torsional eigenfunctions with a single

node (recognized as responsible for significant stresses due to their twisting effect) correspond to the second eigenfunctions of the two Dirichlet problems on the lateral spans. As a result, the dangerous torsional oscillations may arise on *two different* spans and extend across a *longer* portion of the deck (with a total length of $8\pi/5$), potentially leading to greater criticality when wishing to prevent the twisting effect on the structure. In contrast, selecting $a = \frac{1}{2}$ assures a unique “critical” span (the central one) with a shorter length (equal to π). Obviously, to provide a more comprehensive stability assessment for the considered structure, also the *vertical* eigenvalues have to be considered. A full stability analysis will be left for future investigations.

We conclude the paper with another statement following from Theorem 4.1, which extends the results of Corollary 4.3 and Corollary 4.4 to any subsequent eigenvalue. See Fig. 8 for some visual hints. Notice that all the formulas stated in Corollary 4.8 agree with the ones given in Corollary 4.4 for the case $N = 1$.

Corollary 4.8 *Let $0 < \alpha < 1 < \beta$, $M^0 = a$ and $N \geq 2$. Furthermore, denote by $\bar{p}_i \in \bar{P}_{\alpha,\beta}$ a maximizer for (6), for any $i \geq 1$. The following facts hold:*

- (i) *if $0 < a < a_N^\pm$, then for all $1 \leq i \leq N$ one has $\Lambda_i(a) = \Lambda_i^\pm(a)$ and $\bar{p}_i = p_i^\pm$ a.e. in I^\pm . Moreover,*

$$\Lambda_{N+1}(a) = \min\{\Lambda_1^0(a), \Lambda_{N+1}^\pm(a)\} = \begin{cases} \frac{4(N+1)^2\gamma}{(1-a)^2} & \text{if } 0 < a < \min\left\{\frac{1}{2N+3}, a_N^\pm\right\} \\ \frac{\gamma}{a^2} & \text{if } \frac{1}{2N+3} \leq a < a_N^\pm, \end{cases}$$

so that for all $0 < \varepsilon < a_N^\pm$,

$$\max_{0 < a \leq a_N^\pm - \varepsilon} \Lambda_{N+1}(a) = \begin{cases} \Lambda_{N+1}(a_N^\pm - \varepsilon) & \text{if } a_N^\pm < \frac{1}{2N+3} \\ \Lambda_{N+1}\left(\frac{1}{2N+3}\right) & \text{if } \frac{1}{2N+3} \leq a_N^\pm; \end{cases}$$

- (ii) *if $a_N^0 < a < 1$, then for all $1 \leq i \leq N$ one has $\Lambda_i(a) = \Lambda_i^0(a)$ and $\bar{p}_i = p_i^0$ a.e. in I^0 . Moreover,*

$$\Lambda_{N+1}(a) = \min\{\Lambda_1^\pm(a), \Lambda_{N+1}^0(a)\} = \begin{cases} \frac{4\gamma}{(1-a)^2} & \text{if } a_N^0 < a \leq \frac{N+1}{N+3} \\ \frac{(N+1)^2\gamma}{a^2} & \text{if } \max\left\{\frac{N+1}{N+3}, a_N^0\right\} < a < 1, \end{cases}$$

so that for all $0 < \varepsilon < 1 - a_N^0$,

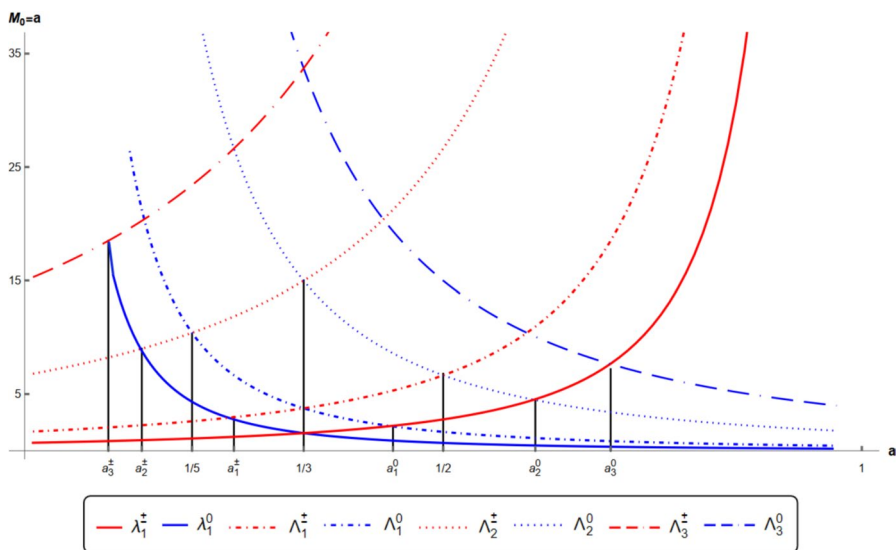


Fig. 8 Plots of the curves $a \mapsto \lambda_1^\pm(a)$, $a \mapsto \Lambda_i^\pm(a)$, $a \mapsto \lambda_1^0(a)$ and $a \mapsto \Lambda_i^0(a)$ for $i = 1, 2, 3$, $M^0 = a$ fixed, $\alpha = \frac{1}{2}, \beta = 2$

$$\max_{a_N^0 + \varepsilon \leq a < 1} \Lambda_{N+1}(a) = \begin{cases} \Lambda_{N+1}\left(\frac{N+1}{N+3}\right) & \text{if } a_N^0 \leq \frac{N+1}{N+3} \\ \Lambda_{N+1}(a_N^0 + \varepsilon) & \text{if } \frac{N+1}{N+3} < a_N^0 < 1. \end{cases}$$

Funding Open access funding provided by Politecnico di Torino within the CRUI-CARE Agreement. The authors are members of the Gruppo Nazionale per l’Analisi Matematica, la Probabilità e le loro Applicazioni (GNAMPA, Italy) of the Istituto Nazionale di Alta Matematica (INdAM, Italy). The research of the first and second authors was carried out within the PRIN 2022 project 2022SLTHCE - Geometric-Analytic Methods for PDEs and Applications GAMPA, funded by European Union - Next Generation EU within the PRIN 2022 program (D.D. 104 - 02/02/2022 Ministero dell’Università e della Ricerca). This manuscript reflects only the authors’ views and opinions and the Ministry cannot be considered responsible for them. The research of the second author is supported also by the MUR grant Dipartimento di Eccellenza 2023-2027 of Dipartimento di Matematica, Politecnico di Milano.

Declarations

Competing Interests The authors have no relevant financial or non-financial interests to disclose.

Open Access This article is licensed under a Creative Commons Attribution 4.0 International License, which permits use, sharing, adaptation, distribution and reproduction in any medium or format, as long as you give appropriate credit to the original author(s) and the source, provide a link to the Creative Commons licence, and indicate if changes were made. The images or other third party material in this article are included in the article’s Creative Commons licence, unless indicated otherwise in a credit line to the material. If material is not included in the article’s Creative Commons licence and your intended use is not permitted by statutory regulation or exceeds the permitted use, you will need to obtain permission directly from the copyright holder. To view a copy of this licence, visit <http://creativecommons.org/licenses/by/4.0/>.

References

1. Gazzola, F.: *Mathematical models for suspension bridges*. Springer, Cham (2015)
2. Berchio, E., Gazzola, F.: A qualitative explanation of the origin of torsional instability in suspension bridges. *Nonlinear Anal.: Theor. Methods Appl.* **121**, 54–72 (2015)
3. Garrione, M., Gazzola, F.: *Nonlinear equations for beams and degenerate plates with piers*. Springer, Cham (2019)
4. Garrione, M., Gazzola, F.: Linear theory for beams with intermediate piers. *Commun. Contemp. Math.* **22**, 1950081 (2020)
5. Berchio, E., Falocchi, A., Garrione, M.: On the stability of a nonlinear nonhomogeneous multiply hinged beam. *SIAM J. Appl. Dyn. Syst.* **20**(2), 908–940 (2021)
6. Henrot, A.: *Extremum problems for eigenvalues of elliptic operators*, *Frontiers in mathematics*, Birkhäuser Verlag, Basel, Boston, Berlin (2006)
7. Krein, M.G.: On certain problems on the maximum and minimum of characteristic values and on the Lyapunov zones of stability. *Am. Math. Soc. Transl.: Series 2*(1), 163–187 (1955)
8. Antunes, P.R.S., Gazzola, F.: some solutions of minimaxmax problems for the torsional displacements of rectangular plates. *ZAMM Z. Angew. Math. Mech.* **98**(11), 1974–1991 (2018)
9. Berchio, E., Buoso, D., Gazzola, F., Zucco, D.: A minimaxmax problem for improving the torsional stability of rectangular plates. *J. Optim. Theory Appl.* **177**, 64–92 (2018)
10. Berchio, E., Falocchi, A.: Maximizing the ratio of eigenvalues of non-homogeneous partially hinged plates. *J. Spectr. Theory* **11**(2), 743–780 (2021)
11. Berchio, E., Falocchi, A.: About symmetry in partially hinged composite plates. *Appl. Math. Optim.* **84**(3), 2645–2669 (2021)
12. Berchio, E., Falocchi, A., Ferrero, A., Ganguly, D.: On the first frequency of reinforced partially hinged plates. *Commun. Contemp. Math.* **23**(3), 1950074 (2021)
13. Berchio, E., Buoso, D., Gazzola, F.: On the variation of longitudinal and torsional frequencies in a partially hinged rectangular plate. *ESAIM Control Optim. Calc. Var.* **24**, 63–87 (2018)
14. Anedda, C., Cuccu, F., Porru, G.: Minimization of the first eigenvalue in problems involving the bi-laplacian. *Revista de Matemática: Teoría y Aplicaciones* **16**, 127–136 (2009)
15. Banks, D.O., Gentry, R.D.: Bounds for functions of eigenvalues of vibrating systems. *J. Math. Anal. Appl.* **51**, 100–128 (1975)
16. Chanillo, S., Grieser, D., Imai, M., Kurata, K., Ohnishi, I.: Symmetry breaking and other phenomena in the optimization of eigenvalues for composite membranes. *Comm. Math. Phys.* **214**, 315–337 (2000)
17. Chen, W., Chou, C.-S., Kao, C.-Y.: Minimizing eigenvalues for inhomogeneous rods and plates. *J. Sci. Comput.* **69**, 983–1013 (2016)
18. Colasuonno, F., Vecchi, E.: Symmetry in the composite plate problem. *Commun. Contemp. Math.* **21**(02), 1850019 (2018)
19. Colasuonno, F., Vecchi, E.: Symmetry and rigidity for the hinged composite plate problem. *J. Differ. Equ.* **266**(8), 4901–4924 (2019)
20. Colbois, B., Provenzano, L.: Eigenvalues of elliptic operators with density. *Calc. Var. Partial Differ. Equ.* **57–36**(2), 36 (2018)
21. Cox, S.J., McLaughlin, J.R.: Extremal eigenvalue problems for composite membranes, I, II. *Appl. Math. Optim.* **22**, 153–167, 169–187 (1990)
22. Cuccu, F., Porru, G.: Maximization of the first eigenvalue in problems involving the bi-Laplacian. *Nonlinear Anal.* **71**, 800–809 (2009)
23. Davoli, E., Mazari, I., Stefanelli, U.: Spectral optimization of inhomogeneous plates. *SIAM J. Control. Optim.* **61**(2), 852–871 (2023)
24. González, M., Lee, K., Lee, T.: Optimal configuration and symmetry breaking phenomena in the composite membrane problem with fractional Laplacian. *J. Differ. Equ.* **274**, 1165–1208 (2021)
25. Lamberti, P.D., Provenzano, L.: A maximum principle in spectral optimization problems for elliptic operators subject to mass density perturbations. *Eurasian Math. J.* **4**(3), 70–83 (2013)
26. Holubová, G., Nečesal, P.: The Fučík spectra for multi-point boundary-value problems. *Electron. J. Diff. Eq. Conf.* **18**, 33–44 (2010)

-
27. Podolny, W.: *Cable-suspended bridges*, In: Structural Steel Designer's Handbook: AISC, AASHTO, AISI, ASTM, AREMA, and ASCE-07 Design Standards. By Brockenbrough, R.L., Merritt, F.S. 5th Edition, McGraw-Hill, New York (2011)

Publisher's Note Springer Nature remains neutral with regard to jurisdictional claims in published maps and institutional affiliations.